International Journal of Computer Networks and Applications (IJCNA)
DOI: 10.22247/ijcna/2023/223692 Volume 10, Issue 6, November – December (2023)

RESEARCH ARTICLE

An Energy-Conserved Stability and Density-Aware QoS-Enabled Topological Change Adaptable Multipath Routing in MANET

Binuja Philomina Marydasan
Department of Computer Science, KSG College of Arts and Science, Coimbatore, Tamail Nadu, India.
binuja02phd@gmail.com

Ranjith Nadarajan
Department of Computer Science, KSG College of Arts and Science, Coimbatore, Tamail Nadu, India.
ranjithksg@gmail.com

Received: 23 August 2023 / Revised: 07 November 2023 / Accepted: 15 November 2023 / Published: 30 December 2023

Abstract – One of the major challenges in Mobile Ad Hoc Networks (MANETs) is achieving Quality-of-Service (QoS) for data communication using multi-disjoint routing protocols. As a result, a Reliable and Stable Topological change Adaptive Ad Hoc On-demand Multipath Distance Vector (RSTA-AOMDV) routing protocol has been designed to select forwarding nodes based on the node's local information. However, this protocol did not consider the node's global stability, and predicting network topology in high-speed MANETs was difficult due to the random movement of nodes. Therefore, this article proposes a novel routing protocol to choose stable nodes and optimal routes for effective data transmission in high-speed MANETs. First, an Energy-conserved Stability and Density-aware QoS-enabled Topological change Adaptable Multipath Routing (ESDQTMR) protocol is developed to ensure data transmission stability from the source to the target nodes by considering both local and global stability factors. Stable Betweenness Centrality (SBC) and transferring packets according to the locality dependency energy level are adopted to find a stable node. After that, an Optimized ESDQTMR (OESDQTMR) protocol is proposed, which uses the Golden Eagle Optimization (GEO) algorithm to choose the best path according to the new objective function. Additionally, fractional calculus is considered to enhance the exploration of the optimal routing path. Finally, extensive simulation findings show that the OESDQTMR protocol achieves greater network performance compared to other routing protocols under varying numbers of nodes and node mobility.

Index Terms – High-Speed MANET, RSTA-AOMDV, Stable Routing, Betweenness Centrality, Optimal Path Selection, Golden Eagle Optimization.

1. INTRODUCTION

MANETs are a distributed framework that involves nodes moving, interacting, and having throughput constraints [1-2]. These networks have various applications, including military, welfare, monitoring, and disaster management systems [3]. However, the network's maximum QoS is often unsatisfactory due to external and internal issues such as link damage, energy exhaustion, traffic problems, and operational issues [4]. The mobility of nodes and energy loss both affect network stability and QoS performance [5]. Therefore, network management is crucial to ensure efficient transmission when resources are scarce. To address these problems, it is important to explore routing algorithms in MANET that can adapt to changing network topologies and limited resources [6-7].

Traditional single-route routing protocols like Ad-hoc On-Demand Distance Vector (AODV) [8] and Dynamic Source Routing (DSR) [9] determine the shortest route from a source to target nodes using constrained resources. However, the fastest and most reliable route may not always be the shortest one. Some routing protocols incorporate additional factors, such as available bandwidth [10], residual energy [11], and link stability [12], to improve route discovery methods. On the other hand, multipath routing with alternate routes provides more stable communication in MANETs with highly variable node movement. By considering alternative routes, many routes can quickly adapt to node or link damage and re-establish data transmission. This approach enhances failure resilience, throughput, and traffic balancing. Over the years, multipath routing algorithms have evolved to meet the increasing demand for better QoS support [13]. These protocols analyse the resources available through alternate paths and select the best path for data transmission based on factors like available bandwidth, idle queue size, and energy range. In recent years, route decision-making in MANET has focused on both routing reliability and the resources available to nodes in the route [14]. However, the routing algorithm for variable path conditions in situations with high-speed movement of resource-limited nodes has not been thoroughly explored. Therefore, it is crucial to develop a MANET routing

RESEARCH ARTICLE

algorithm that can adapt to changes in network structure and support QoS to overcome these challenges.

Accordingly, Chen et al. [15] developed the **T**opological change **A**daptive-AOMDV (TA-AOMDV) routing algorithm to address the challenges of high-mobility networks while ensuring QoS. The TA-AOMDV algorithm incorporates a reliable route selection strategy that aims to minimize route transition delay by considering factors such as residual energy, throughput, queue length, and the likelihood of reliable paths between nodes. Furthermore, the algorithm utilizes a method for estimating link failure, which allows for adjustments to the routing plan based on intermittent probabilistic measurements of link reliability. The TA-AOMDV algorithm has been successfully implemented as a solution for high-mobility MANETs with QoS and resource constraints. However, it is worth noting that the study did not report the path reliability associated with node density, which is crucial for optimal and stable path selection.

To address this issue, a routing protocol called RSTA-AOMDV [16] has been developed. This protocol allows the source node to send data packets to the target node through multiple hops. The selection of successful forwarding nodes is based on the Destination Region Selection (DRS) and Weighted Closeness and Connectivity (WCC) metrics. However, the efficiency of the network was affected during the discovery process of nearby nodes due to the high density and congestion. So, a forwarding node selection strategy was implemented. This strategy utilizes the Request To Send (RTS)/Clear To Send (CTS) transmission to elect the forwarding node by the source node.

1.1. Problem Statement

The issues examined in this study are as follows:

- The RSTA-AOMDV routing protocol did not consider the stability of local and global nodes when selecting the next-hop forwarder node. Consequently, it may not always choose the most stable or reliable node for data forwarding, which could impact network performance and reliability.
- Furthermore, predicting the network's structure proved to be a challenge due to the unpredictable mobility of nodes in high-speed MANET scenarios. The nodes' erratic movement made it difficult to anticipate the network's configuration at any given time, thereby complicating the process of making efficient routing decisions.

1.2. Major Contributions

Therefore, this manuscript proposes a novel routing protocol to address the challenges faced in high-speed MANETs. The protocol, called ESDQTMR, focuses on ensuring stable data transmission between source and destination nodes by considering both local and global stability factors. To identify robust nodes, the protocol utilizes the SBC and routes packets based on the energy levels of the nodes. Additionally, the protocol takes into account packet retransmission time to minimize network overhead. Furthermore, the manuscript introduces the OESDQTMR protocol, which incorporates a best route selection algorithm to create multiple disjoint routes and identify the optimal path for data transmission. The path selection problem is formulated as an optimization problem and solved using the GEO algorithm. The algorithm incorporates a new objective function that utilizes various network parameters to identify the best route among the available options. Fractional calculus is employed to enhance the exploration of the optimal routing path. Overall, the OESDQTMR protocol aims to maximize data transmission reliability in high-speed MANETs by identifying an optimal path with superior network performance.

The remaining paper is structured as follows: Section 2 provides a discussion of previous research related to this study. Section 3 elaborates on the ESDQTMR and OESDQTMR protocols. Section 4 presents the simulation performance. Finally, Section 5 concludes the study and suggests potential future improvements.

2. LITERATURE SURVEY

Zhang and Yang [17] proposed Stable Backup Routing (SBR) to create stable backup paths using Medium Access Control (MAC) signals and considering bit error rates. Qualified backup paths are classified with different priorities for restoring failed paths. However, distributed MANET lacks improvements in transfer latency and network throughput.

Sirmollo and Bitew [18] developed MARA, a routing algorithm that allows nodes to retransmit or reject packets based on velocity, distance, and remaining power. These factors are included in Route REQuest (RREQ) and Route REPly (RREP) procedures to reduce link failure and transfer storm issues. However, link quality and routing load should be considered for better network performance. Kumar & Kukunuru [19] proposed an energy-efficient multipath routing algorithm in MANET using simulated annealing. Routing was based on route and link costs determined by node factors. However, data loss led to decreased Packet Delivery Ratio (PDR).

Velusamy et al. [20] developed a multi-objective node-disjoint multipath routing algorithm in MANETs. However, the routing overhead remained high due to excessive control packet transmission. Wang [21] proposed a genetic algorithm-based multipath routing algorithm that considered distance among nodes. However, it only focused on distance and energy consumption, neglecting the importance of link factors in finding a stable path.

RESEARCH ARTICLE

Naseem et al. [22] developed an Energy-Efficient Load-Balanced AOMDV (EE-LB-AOMDV) routing algorithm to balance the load among each available path according to hop count, round-trip interval, and remaining power. But increasing the node speed, led to more path failures and discoveries. Benatia et al. [23] designed a novel Reliable Multipath routing method depending on link Quality and Stability in urban areas (RMQS-ua) to elect a path that contains good link efficiency and multiple robust links to ensure reliable data transfer. But the other metrics like energy, bandwidth, etc., were needed to integrate for increasing the network performance.

Alghamdi [24] developed a Cuckoo Energy-Efficient Load-Balancing on-demand multipath Routing Protocol (CEELBRP). It uses cuckoo search to select the best routing path based on node power. It also replaces broken paths with idle routes that have higher remaining power during route maintenance. However, this protocol primarily focuses on remaining power during route formation and does not efficiently enhance network performance considering other factors.

Sharma and Tharani [25] developed an ACO-based NDLR-MP routing protocol for MANET. Data transfer started after determining the initial route and finding secondary paths. A local path restoration scheme was used to resend traffic when link failure occurred. Paths were found based on minimum hop count and QoS requirements. Jegadeesan et al. [26] proposed a stable path election for adaptive data transfer in MANETs, finding the optimal least-distance routing path driven by queue storage. The data transmission efficiency was enhanced by keeping the data in the queue. However, other QoS factors such as link stability are needed to improve routing performance.

3. PROPOSED METHODOLOGY

This section provides a brief overview of the ESDQTMR and OESDQTMR protocols. The ESDQTMR protocol selects optimal stable forwarding nodes during the route discovery phase by considering both local stability (DRS and WCC [16]) and global stability (SBC) of a node, as shown in Figure 1.

In the path maintenance phase, the OESDQTMR protocol utilizes the fractional calculus-based GEO algorithm to select the best disjoint path from all available routes. The subsequent sections provide a detailed explanation of the global stability measure and the fractional calculus with the GEO algorithm.

3.1. Efficient Node Stable Routing for Optimal Stable Forwarding Node Selection

Considering the MANET is expressed as a graph $G(V,E)$, where E is the group of links and V is the group of nodes, an adjacency matrix $A=\left(a_{xy}\right)$ that translates the entire network structure: $a_{xy}=1$ when a connection from node x to node y is exist, and $a_{xy}=0$ or else.

It is considered that the MANET comprises N nodes, so $x,y\in\{1,\ldots,N\}$, and A is utilized to calculate the node centrality. Therefore, the Betweenness Centrality (BC) of a node u is defined by equation (1).

$$BC(u)=\sum_{a\neq b\neq u\in V}\frac{\sigma_{a,b}(u)}{\sigma_{a,b}} \quad (1)$$

In equation (1), $\sigma_{a,b}(u)$ is the count of shortest routes from a to b that traverse via u, and $\sigma_{a,b}$ indicates the count of shortest routes from a to b.

An adapted centrality notion called SBC is applied to accurately measure the node stability in a dynamic scenario, which is represented by the remaining energy, link efficiency, and hop count. Therefore, a regularized weighted A is applied to calculate the node's centrality, each element in the matrix is allocated weight with 3 factors such as link quality, the mean remaining energy of the node pair, and the expected hop count. The pairwise weighted A is defined by equation (2).

$$A_w=\begin{pmatrix} w_{11} & w_{12} & \cdots & w_{1N}\\ w_{21} & w_{22} & \cdots & w_{2N}\\ \vdots & \vdots & \ddots & \vdots\\ w_{N1} & w_{N2} & \cdots & w_{NN}\end{pmatrix} \quad (2)$$

In equation (2), $w_{xx}=0, w_{xy}=\beta_1 LQ_{xy}+\beta_2 Meanresenergy_{xy}+\frac{\beta_3}{Expeced\ hop\ count_j}$, where LQ is the link quality, and $Meanresenergy$ is the mean remaining energy of node pairs. Also, β_1,β_2, and β_3 are normalized factors. Therefore, the SBC of u is defined by equation (3).

$$SBC(u)=\sum_{a\neq b\neq u\in V}\frac{\sigma st_{a,b}(u)}{\sigma st_{a,b}} \quad (3)$$

Therefore, the SBC of a node is calculated as a measure of global stability, while the WCC [16] is calculated to determine the local stability and select the most suitable stable forwarding nodes in high-speed MANETs.

3.2. Optimized ESDQTMR for Best Disjoint Path Selection

After implementing the ESDQTMR protocol, equation (4) represents the formation of multiple disjoint routes.

$$R(u,v)=\{r_1(u,v),\ldots,r_l(u,v)\} \quad (4)$$

In equation (4), l denotes the sum amount of disjoint routes formed, and $r_x(u,v)$ defines x^{th} path available between nodes u and v. The optimal route must be selected from these separate routes based on minimum delay, energy usage, and distance. As a result, the fitness function for each separate route is outlined in the following section.

RESEARCH ARTICLE

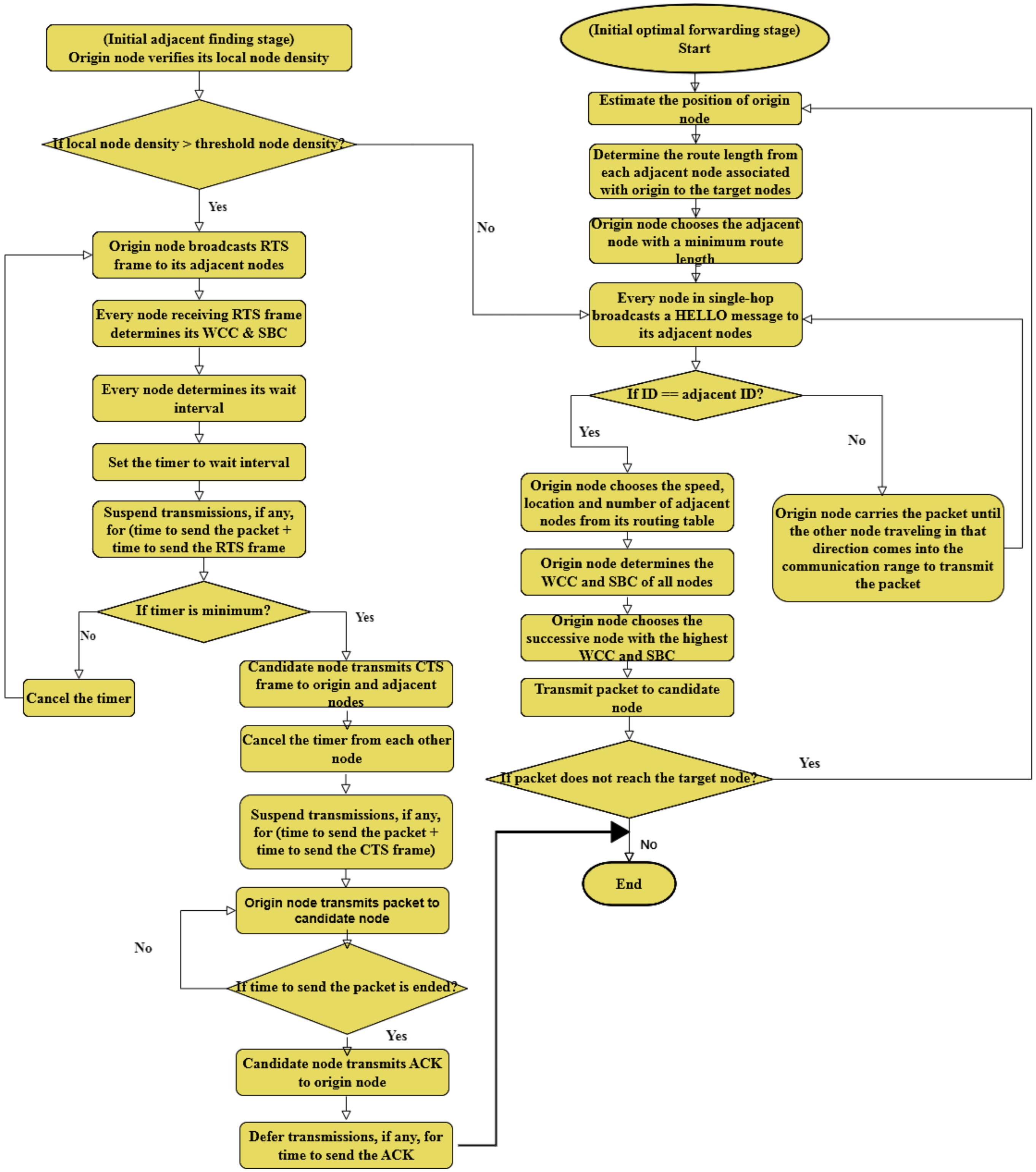

Figure 1 Flow Diagram of ESDQTMR Protocol

RESEARCH ARTICLE

Fitness Function: It is employed to identify the optimal route for data transmission in high-speed MANETs. It can be calculated based on the delay, energy, and distance between nodes, as represented by equations (5) and (6):

$$fitness\ of\ a\ path\ (F) = \sum_{i=1}^{l} \sum_{j=1}^{N_i} f_{ij} \quad (5)$$

$$f_{ij} = \frac{w_1 f_{ij}^{D} + w_2 f_{ij}^{E} + w_3 f_{ij}^{DL}}{3} \quad (6)$$

In equations (5) & (6), N_i is the amount of nodes that exist within the i^{th} route, and w_1, w_2, w_3 are the weight values of corresponding fitness values, such that $w_1 + w_2 + w_3 = 1$. Initially, the distance among nodes in the routing path $\left(f_{ij}^{D}\right)$ is determined by equation (7).

$$f_{ij}^{D} = \frac{1}{(N_i - 1)MD} \sum_{q=1}^{N_i - 1} dist(q, q+1) \quad (7)$$

In equation (7), $dist(q, q+1)$ represents the distance between any two nodes, which exist within a certain disjoint route, MD is the maximum distance from the source to the target nodes. The overall energy use of nodes $\left(f_{ij}^{E}\right)$ in the elected best disjoint route is determined by equation (8).

$$f_{ij}^{E} = \sum_{j=1}^{N_i} \left(1 - E\left(N_j\right)\right) \quad (8)$$

In equation (8), $E\left(N_j\right)$ is the energy utilization of the j^{th} node that exists in the elected disjoint route. Also, the delay between the nodes is determined by equation (9).

$$f_{ij}^{DL} = \sum_{j=1}^{N_i} \frac{f_{ij}^{D} \times N_j}{n} \quad (9)$$

In equation (9), n denotes the sum amount of nodes in the MANET. So, the best disjoint route is elected according to the minimum F, i.e. lower values of delay, energy utilization, and distance among nodes exist within that route. In this study, a fractional GEO algorithm is introduced to determine the optimal routing path. Fractional calculus is utilized due to its ability to adaptively restore results with irreversibility and basic storage features. The exploration (cruise) and exploitation (attack) processes involved in the fractional GEO algorithm are discussed in detail below.

3.2.1. GEO Algorithm

The golden eagle's ability to adjust its speed at various points along its spiral trajectory during hunting serves as a significant inspiration for the GEO algorithm. During the initial stages of hunting, the eagles tend to cruise around and search for potential prey. However, as they progress, they become more inclined to launch an attack. This adaptive behavior allows them to optimize their search for the most promising victim within a feasible area, enabling them to efficiently identify the global best option and avoid getting stuck in local best solutions. The GEO algorithm can be represented by the following model:

- Spiral Trajectory of Golden Eagles

GEO depends on a spiral movement of golden eagles. Every golden eagle may recall its most memorable destination. The eagle wants both to attack its victim and to cruise around in search of the more attractive victim (optimal disjoint route). In all iterations, all golden eagle i arbitrarily chooses the victim of the other eagle j and ring near the most memorable destination by j. As well, i will decide to circle its remembrance (memory); so $j \in \{1, \dots, PS\}$, where PS is the population size.

- Selection of Victim

Golden eagles select a victim for tasks and remember their optimal result. Search agents choose a victim from the group's remembrance. Attack and cruise vectors are determined for the chosen victim. If a new place is better, the remembrance is adjusted. In GEO, the choice of victim is crucial. Golden eagles select their victims based on remembrance. To ensure efficient travel, a one-to-one representation is used, where each golden eagle randomly chooses a victim from the remembrance of another group member. Each victim is assigned to a specific golden eagle. Then, all golden eagles carry out attack and cruise tasks on their chosen victim.

- Attack

The attack is designed through a vector beginning from the present place of the golden eagle and concluding in the place of the victim in the eagle's remembrance. The attack vector for i $\left(\vec{A}_i\right)$ is computed by equation (10).

$$\vec{A}_i = \vec{X}_j^{*} - \vec{X}_i \quad (10)$$

In equation (10), $\vec{X}_j^{*}$ is the optimal place (victim) visited so far by j, and $\vec{X}_i$ denotes the present place of i. The exploitation phase of GEO is highlighted by the attack vector since it concentrates the golden eagle individuals in high-traffic areas.

- Cruise

The attack vector determines the cruise vector, which is tangent to the circle and vertical to the attack vector. The cruise vector in n-dimensions is positioned in the tangent hyperplane to the ring; so, to compute the cruise vector, the formula of the tangent hyperplane should be initially computed. The formula of a hyperplane in n-dimensions is computed by a random location from that hyperplane and a vertical direction to that hyperplane known as a standard vector of the hyperplane. The scalar form of the hyperplane formula in n-dimensional region is shown in equation (11).

$$h_1 x_1 + \dots + h_n x_n = d \Rightarrow \sum_{k=1}^{n} h_k x_k = d \quad (11)$$

In equation (11), $\vec{H} = [h_1, \dots, h_n]$ denotes the standard vector, $X = [x_1, \dots, x_n]$ is the variables vector, $\vec{P} = [p_1, \dots, p_n]$

International Journal of Computer Networks and Applications (IJCNA)
DOI: 10.22247/ijcna/2023/223692 Volume 10, Issue 6, November – December (2023)

RESEARCH ARTICLE

denotes the arbitrary location on the hyperplane, and $d = \vec{H} \cdot \vec{P} = \sum_{k=1}^{n} h_k p_k$. When $\vec{X}_i$ (the place of i) is considered as the arbitrary location in the hyperplane and $\vec{A}_i$ is considered as the standard of the hyperplane, one can demonstrate the hyperplane to which $\vec{C}_i^t$ (the cruise vector for i in iteration t) fits using the equation (12):

$$\sum_{k=1}^{n} a_k x_k = \sum_{k=1}^{n} a_k^t x_k^* \quad (12)$$

In equation (12), $\vec{A}_i = [a_1, \ldots, a_n]$ denotes the attack vector, $X = [x_1, \ldots, x_n]$ indicates the solution vector, and $X^* = [x_1^*, \ldots, x_n^*]$ denotes the place of the chosen victim. Once computing the cruise hyperplane for i in t, a cruise vector for this i within this hyperplane is determined. A golden eagle can select a target location on the cruise hyperplane.

To discover an arbitrary vector on the cruise hyperplane, an arbitrary target location C on this hyperplane is initially found compared to the other, which is previously found (the current place of i). Observe that the beginning location of the cruise vector is the present place of i. As hyperplanes are 1D, an arbitrary $1 \times n$ location is not easily created. An arbitrary location in n-dimensional region is not ensured to be positioned on the cruise hyperplane. A new location positioned on the n-dimensional cruise hyperplane contains $n-1$ levels of choice, defining that $n-1$ dimensions are selected easily, yet the hyperplane formula directs the final dimension as illustrated in equation (11). The final dimension should be selected; thus, it fulfills the hyperplane formula. So, $n-1$ free parameters and single constant parameter are found. Below process is utilized to discover an arbitrary n-dimensional target location c positioned on the cruise hyperplane for i.

1. Arbitrarily select a single parameter from n parameters as a constant parameter. The index of the chosen parameter is denoted by m. Observe that the constant parameter is not selected from the parameters whose respective component in $\vec{A}_i$ is 0 because if the parameter coefficient in equation (11) is 0, then the hyperplane is parallel to the axis of that parameter and that parameter will consider any range for an arbitrary mixture of another $n-1$ parameter.

2. Allocate random values to each variable excluding the m^{th} variable since the m^{th} variable is fixed.

3. Determine the value of the fixed variable as equation (13):

$$c_m = \frac{d - \sum_{k,k \neq m} a_k}{a_m} \quad (13)$$

In equation (13), c_m denotes the m^{th} element of C, a_k denotes the j^{th} element of $\vec{A}_i$, d indicates the right-hand side of the equation (11), a_m denotes the m^{th} element of $\vec{A}_i$, and m denotes the index of a constant parameter. The arbitrary target location on the cruise hyperplane is determined. Equation (14) defines the target location on the cruise hyperplane.

$$\vec{C}_i = \left(c_1 = arbitrary, \ldots, c_m = \frac{d - \sum_{k,k \neq m} a_k}{a_m}, \ldots, c_n = arbitrary\right) \quad (14)$$

After determining the target location, the cruise vector is computed for i in t. The components of the acquired target location are assigned arbitrary values ranging from 0 to 1. The cruise vector is designed to draw the golden eagle individuals towards regions that are different from those in their memory. This emphasizes the search stage of GEO.

- Traveling to Fresh Places

The movement of the golden eagles involves the attack and cruise vectors. The step vector for i in t is described by equation (15).

$$\Delta x_i^t = \vec{r}_1 p_a^t \frac{\vec{A}_i}{\|\vec{A}_i\|} + \vec{r}_2 p_c^t \frac{\vec{C}_i}{\|\vec{C}_i\|} \quad (15)$$

In equation (15), p_a^t denotes the attack coefficient in t, p_c^t denotes the cruise coefficient in t, and modifies how golden eagles are influenced by attack and cruise. Also, $\vec{r}_1$ and $\vec{r}_2$ are arbitrary vectors whose components are in the range 0 and 1. $\|\vec{A}_i\|$ and $\|\vec{C}_i\|$ define the Euclidean term of the attack and cruise vectors, which are determined as equation (16):

$$\|\vec{A}_i\| = \sqrt{\sum_{k=1}^{n} a_k^2} \text{ and } \|\vec{C}_i\| = \sqrt{\sum_{k=1}^{n} c_k^2} \quad (16)$$

The location of the golden eagles in $t+1$ is computed by including Δx_i^t to the places in t as equation (17):

$$x^{t+1} = x^t + \Delta x_i^t \quad (17)$$

When the objective of a fresh place of i is superior to the place in its remembrance, the remembrance of i is modified by the fresh place. When the fitness of both places is equal, selecting the ideal place becomes problematic. To address this issue, the GEO algorithm incorporates fractional calculus. In cases where the fitness of both places is equal, the solution of both places yields an equal value as shown in equation (18):

$$x^{t+1} = x^t \quad (18)$$

To change the order of the solution formula, the outcomes of x^{t+1} is reorganized as equation (19):

$$x^{t+1} - x^t = 0 \quad (19)$$

Here, x^{t+1} is taken as the discrete form of the derivative of $\alpha_F = 1$ that provides equation (20).

$$D^{\alpha_F}[x^{t+1}] = 0 \quad (20)$$

To elect the best route, the range of α_F is altered between 0 and 1. After that, the difference and impact of remembrance are sustained by fractional calculus. Equation (19) is rewritten using the second-order derivative functions:

$$x^{t+1} - \alpha_F x^t - \frac{1}{2}\alpha_F x^t = 0$$

$$x^{t+1} = \alpha_F x^t - \frac{1}{2}\alpha_F x^t \quad (21)$$

In equation (21), x^{t+1} denotes the final solution (place) created from the fractional calculus scheme, which is elected as the best-visited place by discarding other weak solutions. The eagle moves, but remembrance remains. In the next iteration, golden eagles select one from the population to circle its memorable place, compute vectors, and find a fresh place. This process continues until the stopping condition is met.

- Switch From Search to Exploitation

This optimizer explores in the first iterations and exploits in the final iterations because golden eagles cruise in the early stages of the search and attack in the end. The GEO utilizes p_a and p_c to change from search to exploitation. The process begins with minimum p_a and maximum p_c. As the iterations continue, p_a is slowly raised when p_c is slowly reduced.

An early and last range of both factors is set by the system. Intermediary ranges are computed by the linear shift as equation (22):

$$\begin{cases} p_a = p_a^0 + \frac{t}{T}|p_a^T - p_a^0| \\ p_c = p_c^0 + \frac{t}{T}|p_c^T - p_c^0| \end{cases} \quad (22)$$

In equation (22), t is the present iteration, T is the highest iteration, p_a^0 and p_a^T define the early and last ranges of the tendency to attack (p_a), correspondingly, and p_c^0 and p_c^T define early and last ranges of the tendency to cruise (p_c), correspondingly.

Based on these notions, the pseudocode for selecting the optimal path using the GEO is given in Algorithm 1.

Input: l number of disjoint routes formed by ESDQTMR protocol

Output: Optimal disjoint path

1. Begin
2. Set the population size n, the maximum iterations T, and parameter m;
3. Initialize the population of golden eagles (number of disjoint routes formed by ESDQTMR) and the population remembrance;
4. Initialize $\mathrm{p_a}$ and $\mathrm{p_c}$;
5. Evaluate the fitness function by equation (5)
6. for
7. $(\mathrm{t} < \mathrm{T})$Update $\mathrm{p_a}$ and $\mathrm{p_c}$ by equation (22);
8. $\mathrm{for}(\mathrm{i} = 1{:}\,\mathrm{n})$
9. Choose a victim randomly from the population's remembrance;
10. Compute the attack vector $\vec{\mathrm{A}}$ using equation (10);
11. $\mathrm{if}(\text{attack vector's length} \neq 0)$
12. Compute the cruise vector $\vec{\mathrm{C}}$ by equations (11) – (14);
13. Compute the step vector $\Delta\mathrm{x}$ by equations (15) – (16);
14. Update new place by equation (17);
15. Evaluate the fitness function for the new place;
16. $\mathrm{if}(\text{fitness of the new place} > \text{fitness of the place in i's memory})$
17. Swap the fresh place with the place in i's remembrance;
18. $\text{else if}(\text{fitness of the new place} = \text{fitness of the place in i's memory})$
19. Use the fractional calculus scheme to find the best place;
20. end if
21. end if
22. end for
23. end for
24. Obtain the best-visited place (victim, i.e., the most optimal route);
25. End

Algorithm 1 Pseudocode for Selecting the Optimal Path Using GEO

Hence, the best disjoint route is elected from the source to the target nodes for data transfer.

4. RESULTS AND DISCUSSION

This section evaluates the efficiency of the ESDQTMR and OESDQTMR protocols in Network Simulator version 2.35 (NS2.35) by simulating them at different node mobility and densities. The network model is created using the simulation parameters outlined in Table 1.

Table 1 Simulation Parameters

Parameter	Range
No. of nodes	10 – 100
Node mobility	0 – 50 m/s

RESEARCH ARTICLE

Simulation region	$1500 \times 1500m^2$
Queue length	50 packet
Routing protocol	AOMDV
MAC layer	IEEE 802.11
Traffic type	Constant Bit Rate (CBR)
Packet size	512 bytes
Data rate	16 Kbps
Communication range	250 m
Mobility model	Random way point
Channel bandwidth	2 Mbps
Carrier frequency	2.4 GHz
Initial energy	100 J
Transmit power	0.6 J
Received power	0.35 J
Simulation period	150 sec

To conduct performance analysis, the existing routing protocols were also simulated using the parameters being considered. The ESDQTMR and OESDQTMR protocols were evaluated against RSTA-AOMDV [16], EE-LB-AOMDV [22], CEELBRP [24], and ACO-NDLR-MP [25]. The efficiency of these protocols was assessed by measuring the following metrics:

- End-to-End Delay (E2E-D): It refers to the interval consumed for data transmission between a source and target node. It is calculated in equation (23).

$$E2E - D = \sum_{i=0}^{n}\left(t_i^{received} - t_i^{transmit}\right)/_n \quad (23)$$

In equation (23), n indicates the quantity of successfully delivered data, $t_i^{received}$ defines the interval at which i^{th} data is delivered at the destination and $t_i^{transmit}$ denotes the interval at which i^{th} data is forwarded from the source node.

- Throughput: It is the quantity of bits that are successfully delivered to the destination within a specific interval. This can be calculated using equation (24).

$$Throughput = \sum_{i=0}^{n} R_i^{Byte} /_{t^{sim}} \quad (24)$$

In equation (24), R_i^{Byte} is an overall quantity of bytes delivered by all nodes and t^{sim} is a simulation interval.

- Normalized Routing Overhead (NRO): It quantifies the ratio of control packets to the total quantity of data packets successfully delivered at the destination. It is calculated by equation (25).

$$NRO = \frac{Total\ number\ of\ control\ packets}{Total\ number\ of\ data\ packets} \times 100\% \quad (25)$$

- PDR: It is the proportion of the delivered data at the target node to the data forwarded from the source node. It is calculated in equation (26).

$$PDR = \frac{Total\ number\ of\ packets\ received\ by\ the\ target}{Number\ of\ packets\ transmitted\ by\ origin} \quad (26)$$

Mean Energy Consumption (MEC): It defines an overall energy dissipated by all nodes during data transfer.

4.1. Comparing Network Performance at Different Node Speeds

In this scenario, 50 nodes are distributed in $1500 \times 1500m^2$ area and a CBR of 16Kbps is set. Node speed is 0-50m/s and after 10 seconds of simulation, the node transmits data.

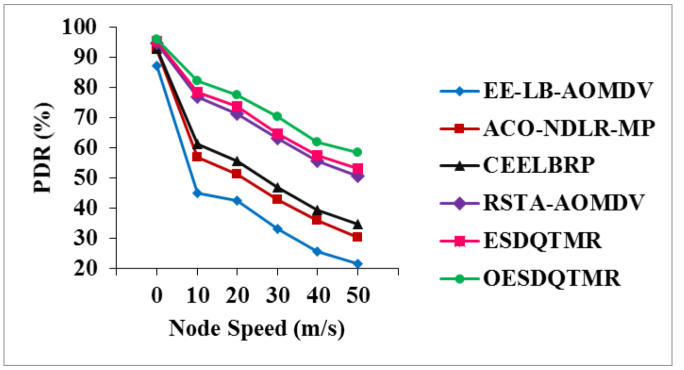

Figure 2 PDR vs. Node Speed

In Figure 2, the PDR values of various routing protocols are plotted for varying node speeds. It is noticed that the OESDQTMR protocol attains maximum PDR when increasing the node speed, in contrast with the other protocols. On average, the PDR of the OESDQTMR protocol is increased by 75.28%, 44.14%, 34.92%, 8.28%, and 5.61% compared to the EE-LB-AOMDV, ACO-NDLR-MP, CEELBRP, RSTA-AOMDV, and ESDQTMR protocols, respectively, due to the selection of both a stable forwarding node and an optimal disjoint path for data transmission.

In Figure 3, the results of the E2E-D for different routing protocols under varying node speeds are presented. It can be observed that the OESDQTMR protocol demonstrates the lowest E2E-D as the node speed increases, in comparison to the other protocols. On average, the E2E-D of the OESDQTMR protocol is reduced by 65.87%, 57.99%, 46.73%, 28.16%, and 20.24% when compared to the EE-LB-AOMDV, ACO-NDLR-MP, CEELBRP, RSTA-AOMDV, and ESDQTMR protocols, respectively, during the transmission of data via the elected optimal disjoint route.

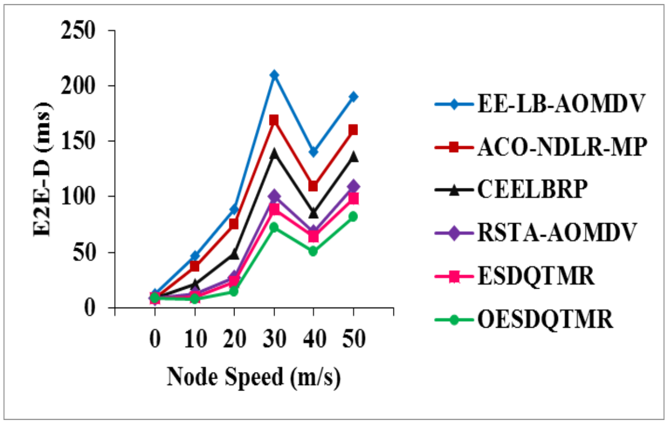

Figure 3 E2E-D vs. Node Speed

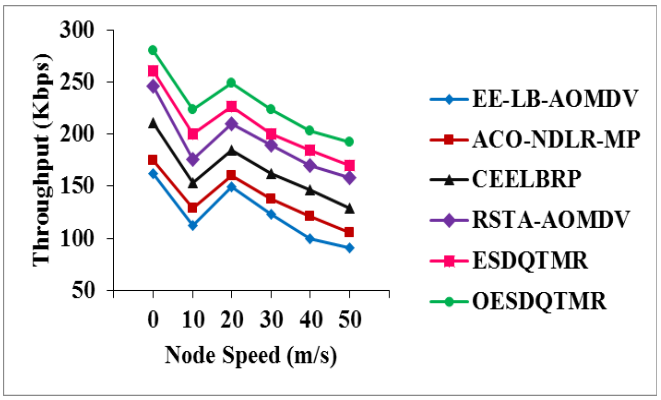

Figure 4 Throughput vs. Node Speed

In Figure 4, throughput ranges of the different routing protocols under varying node speeds are presented. It is shown that the OESDQTMR protocol establishes a higher throughput than the other protocols for different node speeds. On average, the throughput of the OESDQTMR is improved by 86.7%, 65.7%, 39.15%, 19.36%, and 10.38% compared to the EE-LB-AOMDV, ACO-NDLR-MP, CEELBRP, RSTA-AOMDV, and ESDQTMR protocols, respectively.

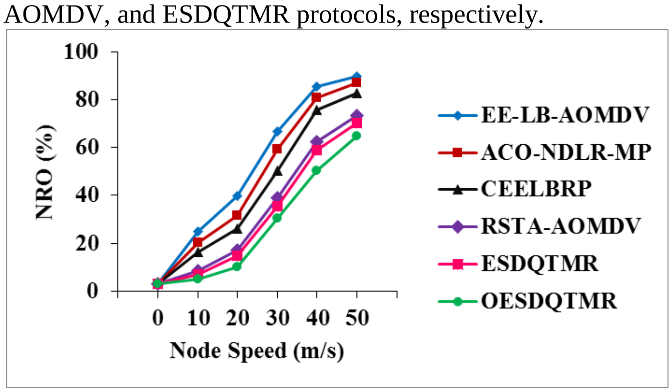

Figure 5 NRO vs. Node Speed

Figure 5 illustrates the NRO values of various routing protocols at different node speeds. It is evident that the OESDQTMR protocol significantly reduces the NRO compared to other protocols across different node speeds. On average, the NRO of the OESDQTMR protocol is reduced by 47.27%, 42.11%, 35.72%, 19.8%, and 13.88% in comparison to the EE-LB-AOMDV, ACO-NDLR-MP, CEELBRP, RSTA-AOMDV, and ESDQTMR protocols, respectively.

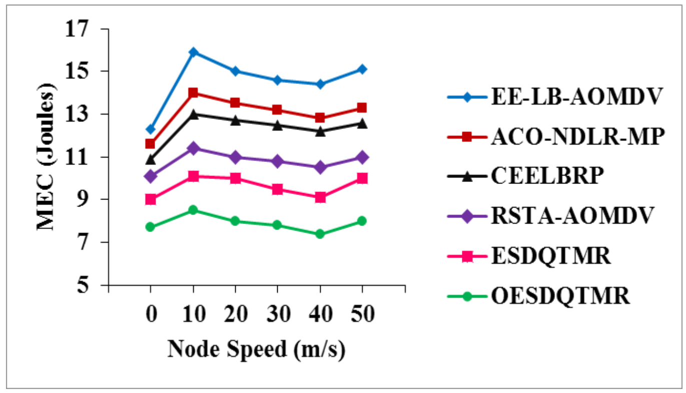

Figure 6 MEC vs. Node Speed

Figure 6 demonstrates the MEC of different routing protocols for various node speeds. It is observed that the OESDQTMR protocol reduces the MEC compared to other protocols at different node speeds. On average, the MEC of the OESDQTMR protocol is reduced by 45.7%, 39.54%, 35.86%, 26.85%, and 17.85% compared to the EE-LB-AOMDV, ACO-NDLR-MP, CEELBRP, RSTA-AOMDV, and ESDQTMR protocols, respectively.

4.2. Comparing Network Performance at Different Node Densities

In this scenario, consider the number of nodes ranging from 10 to 100, which are arbitrarily circulated in $1500 \times 1500m^2$ area. A constant node speed is 10m/s and CBR is 16Kbps.

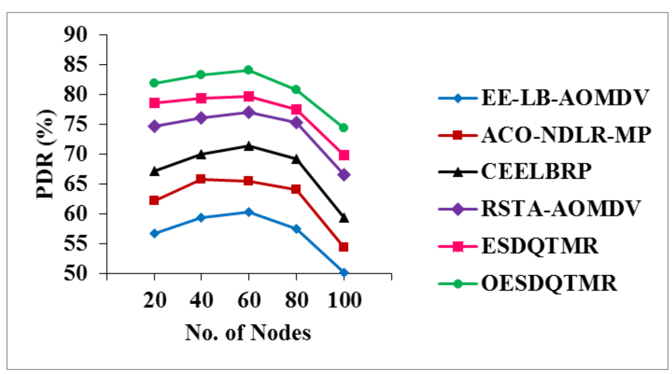

Figure 7 PDR vs. No. of Nodes

Figure 7 shows the PDR values of various routing protocols for different node counts. The OESDQTMR protocol outperforms the other protocols by achieving the highest PDR as the number of nodes increases. On average, the PDR of the OESDQTMR protocol is 42.37%, 29.68%, 19.94%, 9.39%, and 5.1% higher than the EE-LB-AOMDV, ACO-NDLR-MP, CEELBRP, RSTA-AOMDV, and ESDQTMR protocols, respectively.

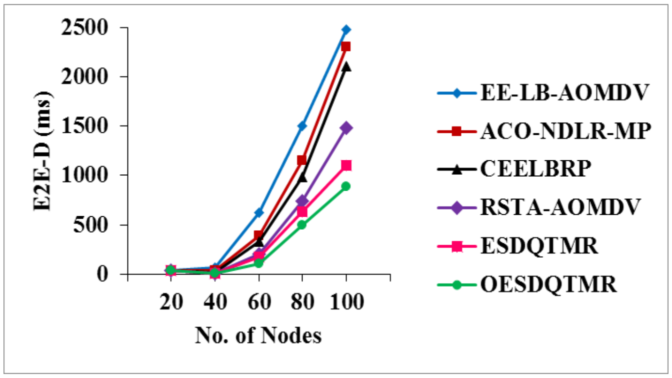

Figure 8 E2E-D vs. No. of Nodes

Figure 8 portrays the E2E-D vs. different numbers of nodes for various routing protocols. It is addressed that the OESDQTMR protocol reduces the E2E-D by 67.42%, 60.94%, 55.99%, 38.25%, and 21.75% over EE-LB-AOMDV, ACO-NDLR-MP, CEELBRP, RSTA-AOMDV, and ESDQTMR protocols, respectively.

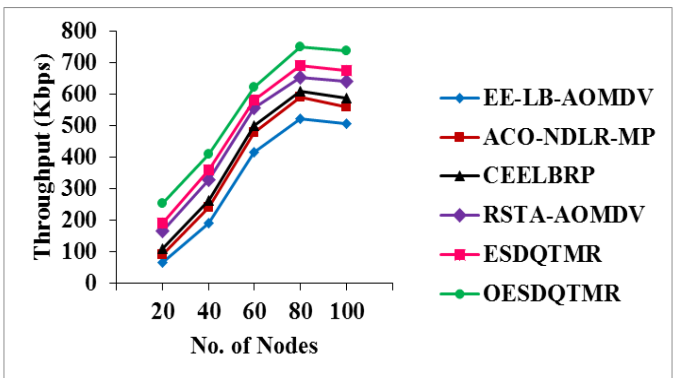

Figure 9 Throughput vs. No. of Nodes

Figure 9 displays the throughput results for various routing protocols under different numbers of nodes. It is observed that the OESDQTMR protocol increases the throughput by 62.95%, 41.55%, 33.8%, 18.42%, and 10.92% over EE-LB-AOMDV, ACO-NDLR-MP, CEELBRP, RSTA-AOMDV, and ESDQTMR protocols, respectively. This is due to the selection of both stable forwarding nodes and optimal disjoint routes for reliable data transmission.

Figure 10 exhibits the NRO of various routing protocols for different node counts. It is noticed that the OESDQTMR protocol decreases the NRO by 61.34%, 53.87%, 48.04%, 28.02%, and 18.93% over the EE-LB-AOMDV, ACO-NDLR-MP, CEELBRP, RSTA-AOMDV, and ESDQTMR protocols, respectively.

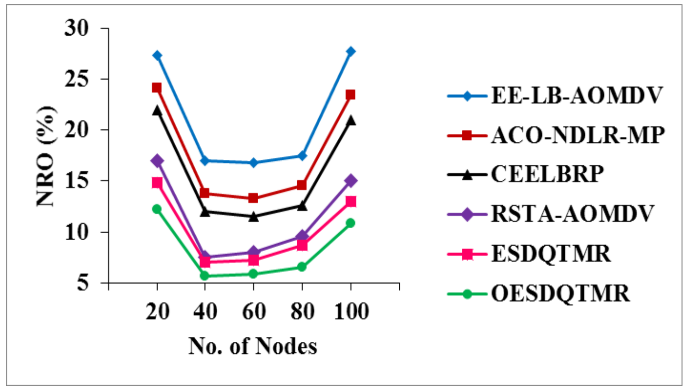

Figure 10 NRO vs. No. of Nodes

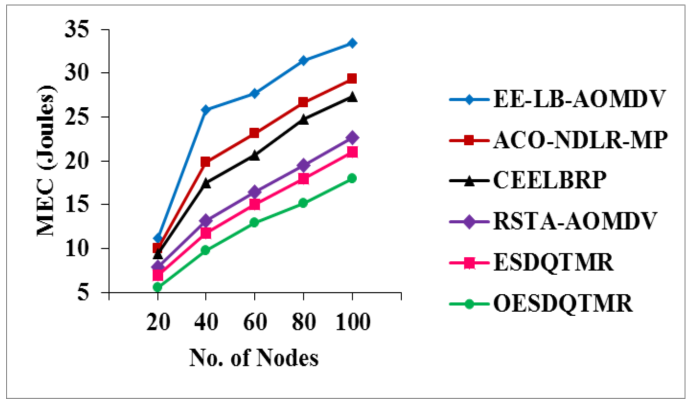

Figure 11 MEC vs. No. of Nodes

Figure 11 depicts the MEC results for various routing protocols with different numbers of nodes. It is observed that the OESDQTMR protocol reduces the MEC by 52.47%, 43.49%, 38.21%, 22.71%, and 15.38% over the EE-LB-AOMDV, ACO-NDLR-MP, CEELBRP, RSTA-AOMDV, and ESDQTMR protocols, respectively.

4.3. Discussion

The analysis suggests that the OESDQTMR protocol improves network performance in both scenarios. This is accomplished by considering local and global node stability factors to select the most stable forwarding nodes in the routing path. As a result, network performance and reliability are enhanced.

Additionally, the GEO algorithm is used to select the most optimal disjoint paths for reliable data transmission in high-mobility MANETs. This leads to efficient routing decisions, resulting in high throughput, high PDR, reduced E2E-D, low NRO, and decreased MEC compared to existing routing protocols.

RESEARCH ARTICLE

5. CONCLUSION

In this study, a new routing protocol was developed for information exchange in high-speed MANETs. Initially, the ESDQTMR protocol was proposed to find stable forwarding nodes based on the SBC and the locality dependency energy degree. Second, this protocol was extended to OESDQTMR by applying the fractional calculus with GEO-based optimal route selection according to the fitness value of each available disjoint route. Finally, the testbed results demonstrated that the OESDQTMR protocol has 82.2% PDR, 7.2ms E2E-D, 224Kbps throughput, 4.9% NRO, and 8.5J MEC if the node speed is 10m/s in the first scenario. Similarly, the OESDQTMR protocol has 74.4% PDR, 886.61ms E2E-D, 738.2Kbps throughput, 10.8% NRO, and 18J MEC, if the number of nodes is 100 in the second scenario, compared to the existing routing protocols.

REFERENCES

[1] Tripathy, B. K., Jena, S. K., Reddy, V., Das, S., & Panda, S. K. (2021). A novel communication framework between MANET and WSN in IoT based smart environment. International Journal of Information Technology, 13, 921-931.
[2] Quy, V. K., Nam, V. H., Linh, D. M., & Ngoc, L. A. (2022). Routing algorithms for MANET-IoT networks: a comprehensive survey. Wireless Personal Communications, 125(4), 3501-3525.
[3] Agrawal, R., Faujdar, N., Romero, C. A. T., Sharma, O., Abdulsahib, G. M., Khalaf, O. I., ... & Ghoneim, O. A. (2022). Classification and comparison of ad hoc networks: a review. Egyptian Informatics Journal, 24, 1-25.
[4] Ramalingam, R., Muniyan, R., Dumka, A., Singh, D. P., Mohamed, H. G., Singh, R., ... & Noya, I. D. (2022). Routing protocol for MANET based on QoS-aware service composition with dynamic secured broker selection. Electronics, 11(17), 1-17.
[5] Priyambodo, T. K., Wijayanto, D., & Gitakarma, M. S. (2020). Performance optimization of MANET networks through routing protocol analysis. Computers, 10(1), 1-13.
[6] Soomro, A. M., Fudzee, M. F. B. M., Hussain, M., Saim, H. M., Zaman, G., Atta-ur-Rahman, H. A., & Nabil, M. (2022). Comparative review of routing protocols in manet for future research in disaster management. Journal of Communications, 17(9), 734-744.
[7] Alasadi, S. A., Al-Joda, A. A., & Abdullah, E. F. (2021). Mobile ad hoc network (MANET) proactive and reactive routing protocols. Journal of Discrete Mathematical sciences and Cryptography, 24(7), 2017-2025.
[8] Bamhdi, A. M. (2020). Efficient dynamic-power AODV routing protocol based on node density. Computer Standards & Interfaces, 70, 1-16.
[9] Prasath, N., & Sreemathy, J. (2019). Optimized dynamic source routing protocol for MANETs. Cluster Computing, 22(Suppl 5), 12397-12409.
[10] Sharma, A., Bansal, A., & Rishiwal, V. (2020). SBADR: stable and bandwidth aware dynamic routing protocol for mobile ad hoc network. International Journal of Pervasive Computing and Communications, 16(3), 205-221.
[11] Tilwari, V., Dimyati, K., Hindia, M. N., Fattouh, A., & Amiri, I. S. (2019). Mobility, residual energy, and link quality aware multipath routing in MANETs with Q-learning algorithm. Applied Sciences, 9(8), 1-23.
[12] Ghafouri vaighan, M., & Jabraeil Jamali, M. A. (2019). A multipath QoS multicast routing protocol based on link stability and route reliability in mobile ad-hoc networks. Journal of ambient intelligence and humanized computing, 10(1), 107-123.
[13] Mohsin, A. H. (2022). Optimize routing protocol overheads in MANETs: challenges and solutions: a review paper. Wireless Personal Communications, 126(4), 2871-2910.
[14] Alkhamisi, A. O., Buhari, S. M., Tsaramirsis, G., & Basheri, M. (2020). An integrated incentive and trust-based optimal path identification in ad hoc on-demand multipath distance vector routing for MANET. International Journal of Grid and Utility Computing, 11(2), 169-184.
[15] Chen, Z., Zhou, W., Wu, S., & Cheng, L. (2020). An adaptive on-demand multipath routing protocol with QoS support for high-speed MANET. IEEE Access, 8, 44760-44773.
[16] Marydasan, B. P., & Nadarajan, R. (2022). Topology change aware on demand routing protocol for improving reliability and stability of MANET. International Journal of Intelligent Engineering & Systems, 15(4), 468-478.
[17] Zhang, F., & Yang, G. (2020). A stable backup routing protocol for wireless ad hoc networks. Sensors, 20(23), 1-11.
[18] Sirmollo, C. Z., & Bitew, M. A. (2021). Mobility-aware routing algorithm for mobile ad hoc networks. Wireless Communications and Mobile Computing, 2021, 1-12.
[19] Kumar, C. N., & Kukunuru, N. (2021). Energy efficient disjoint multipath routing protocol using simulated annealing in MANET. Wireless Personal Communications, 120(2), 1027-1042.
[20] Velusamy, B., Karunanithy, K., Sauveron, D., Akram, R. N., & Cho, J. (2021). Multi-objective function-based node-disjoint multipath routing for mobile ad hoc networks. Electronics, 10(15), 1-17.
[21] Wang, S. (2021). Multipath routing based on genetic algorithm in wireless sensor networks. Mathematical Problems in Engineering, 2021, 1-6.
[22] Naseem, M., Ahamad, G., Sharma, S., & Abbasi, E. (2021). EE-LB-AOMDV: an efficient energy constraints-based load-balanced multipath routing protocol for MANETs. International Journal of Communication Systems, 34(16), 1-13.
[23] Benatia, S. E., Smail, O., Meftah, B., Rebbah, M., & Cousin, B. (2021). A reliable multipath routing protocol based on link quality and stability for MANETs in urban areas. Simulation Modelling Practice and Theory, 113, 1-17.
[24] Alghamdi, S. A. (2022). Cuckoo energy-efficient load-balancing on-demand multipath routing protocol. Arabian Journal for Science and Engineering, 47(2), 1321-1335.
[25] Sharma, A., & Tharani, L. (2022). Ant colony based node disjoint local repair in multipath routing in MANET network. Wireless Personal Communications, 127(1), 159-186.
[26] Jegadeesan, R., Beno, A., Manikandan, S. P., Rao, D. S., Narukullapati, B. K., Kumar, T. R., Omarov, B., & Batu, A. (2022). Stable route selection for adaptive packet transmission in 5g-based mobile communications. Wireless Communications and Mobile Computing, 2022, 1-10.

Authors

Binuja Philomina Marydasan completed B.Sc. Computer Science (2011) from Bharathiar University, Coimbatore, India and Master of Networking Technology (2013) from Karunya University, Coimbatore, India. Currently pursuing Ph.D. in Computer Science at KSG College of Arts and Science, Coimbatore, India. Interested Research area is networking.

RESEARCH ARTICLE

Dr. Ranjith Nadarajan is currently working as Assistant Professor and Head of the Department of Computer Application at KSG College of Arts and Science ,Coimbatore. He has Completed B.SC Computer Science(2005) from Annamalai University ,Coimbatore ,India. Master's degree in Master of Information Technology(2008) at Sikkim Manipal, Manipal and Master of computer Application(2011)at Periyar university, Salem, India and D.C.Tech at TRNP, Dharapuram and many diploma certified courses, SWAYAM and NAPTEL Courses. Ph.D.(2018) at Karpagam University, Coimbatore, India. He was working as software Developer in various IT industries. He has 13 years of working experience in teaching.

How to cite this article:

Binuja Philomina Marydasan, Ranjith Nadarajan, "An Energy-Conserved Stability and Density-Aware QoS-Enabled Topological Change Adaptable Multipath Routing in MANET", International Journal of Computer Networks and Applications (IJCNA), 10(6), PP: 964-975, 2023, DOI: 10.22247/ijcna/2023/223692.